Available online at www.sciencedirect.com
SCIENCE DIRECT
Biochemical Pharmacology 70 (2005) 1288–1297
Biochemical Pharmacology
www.elsevier.com/locate/biochempharm

The ribonucleotide reductase subunit M2B subcellular localization and functional importance for DNA replication in physiological growth of KB cells

Xiyong Liu, Bingsen Zhou, Lijun Xue, Jennifer Shih, Karen Tye, Christina Qi, Yun Yen *

Department of Medical Oncology and Therapeutic Research, City of Hope National Medical Center, 1500 E. Duarte Road, Duarte, CA 91010-3000, USA

Received 31 May 2005; accepted 10 August 2005

Abstract

Ribonucleoside diphosphate reductase (EC 1.17.4.1) (RR) is a potential target for antineoplastic agents due to its crucial role in DNA replication and repair. The expression and activity of RR subunits are highly regulated to maintain an optimal dNTP pool, which is required to maintain genetic fidelity. The human RR small subunit M2B (p53R2) is thought to contribute to DNA repair in response to DNA damage. However, it is not clear whether M2B is involved in providing dNTPs for DNA replication under physiological growth conditions. Serum starvation synchronized studies showed that a rapid increase of M2B was associated with cyclin E, which is responsible for regulation of G_1/S-phase transition. A living cell sorting study that used KB cells in normal growth, further confirmed that M2B increased to maximum levels at the G_1/S-phase transition, and decreased with DNA synthesis. Confocal studies revealed that M2B redistributed from the cytoplasm to the nucleus earlier than hRRM2 in response to DNA replication. Nuclear accumulation of M2B is associated with dynamic changes in dNTP at early periods of serum addition. By using M2B-shRNA expression vectors, inhibition of M2B may result in growth retardation in KB cells. We conclude that M2B may translocate from the cytoplasm into the nucleus and allow dNTPs to initiate DNA synthesis in KB cells under physiological conditions. Thus, our findings suggested that M2B might play an important role for initiating DNA replication of KB cells in normal growth.

Keywords: Ribonucleotide reductase; DNA replication; Cell cycle; Cell proliferation; Small interference RNA; Subcellular localization

1. Introduction

Ribonucleoside diphosphate reductase (EC 1.17.4.1) (RR) plays an essential role in converting ribonucleoside diphosphate (NDP) to 2′-deoxyribonucleoside diphosphate (dNDP), which is necessary for DNA synthesis and repair [1]. RR is a potential target for antineoplastic agents due to its crucial roles in cell proliferation and maintaining cell integrity. Hydroxyurea is a widely used chemotherapeutic agent due to its ability to inhibit RR subunit hRRM2 and block cell proliferation.

Expression and activity of RR is highly regulated, both in the cell cycle and at DNA damage checkpoints, to maintain optimal dNTP pools required for genetic fidelity [2]. In eukaryotic cells, large α and small β subunits form an $\alpha_2\beta_2$ heterotetramer that is required for RR activity [1]. There are four RR subunit genes in budding yeast; RNR1 and RNR3 code for large subunits, while RNR2 and RNR4 code for small subunits [3]. For human cells, the large subunit M1 (hRRM1) is a homologue to RNR1, and the small subunit M2 (hRRM2) is a homologue to RNR2 [4]. The recently identified human RR small subunit M2B (p53R2) is 80% identical to subunit M2, but only 60% and 40% identical to RNR2 and RNR4, respectively [4]. The large subunits of the RR holoenzyme possess binding sites for enzyme regulation, whereas the small subunits

Abbreviations: hRR, human ribonucleotide reductase; hRRM1, human ribonucleotide reductase large subunit M1; hRRM2, human ribonucleotide reductase small subunit M2; M2B, a p53-dependent human ribonucleotide reductase small subunit M2B, it also called p53R2; RNR, yeast ribonucleotide reductase; shRNA, short hairpin interference RNA; dNTP, deoxyribonucleoside triphosphate; NDP, ribonucleoside diphosphate; CDP, cytidine 5′-diphosphate; dCDP, deoxycytidine 5′-diphosphate; NLS, nuclear localization sequence; DAPI, 4′,6′-diamidino-2-phenylindole

* Corresponding author. Tel.: +1 626 359 8111x62867; fax: +1 626 301 8233.
E-mail address: yyen@coh.org (Y. Yen).

0006-2952/$ – see front matter © 2005 Elsevier Inc. All rights reserved.
doi:10.1016/j.bcp.2005.08.005

contain non-heme iron centers and tyrosyl free radicals that are involved in RR activity [5].

For yeast, RNR1 and RNR2 are essential for mitotic growth, and RNR3 is highly inducible by genotoxic stress [6]. In mammalian cells, several studies revealed that the small subunit M2 of human (R2 of mouse) is an S-phase-dependent protein that contributes to RR activity in DNA replication and repair [7,8]. The small subunit M2B has been reported to be involved in a p53-dependent cell cycle checkpoint for DNA damage [4,9,10]. M2B expression, rather than hRRM2 can be induced in response to the stress of DNA damage in p53 wild-type cells [9–11]. Impairment of DNA repair in p53 defective cells may be due to the malfunction of p53, which normally induces M2B in response to DNA damage [12]. With a non-lethal dose of UV irradiation, wild-type p53 and hRRM1 can interact with small subunits hRRM2 and M2B, to regulate RR activity through protein-protein interactions [13]. An in vitro assay demonstrated that M2B and hRRM1 could form an hRR holoenzyme [14,15]. Thus, M2B is thought to contribute to DNA repair in response to DNA damage [9], but the functions and contributions of M2B to DNA replication have never been demonstrated under physiological conditions.

Translocation of RR is an important component of cell regulation ability in DNA replication and repair. A readily sedimentable fraction, containing the activities of RR, thymidylate synthetase, DNA polymerase, dihydrofolate reductase and NDP kinase, was extracted from the nucleus of CHEF/18 cells in the S-phase [16]. When cells passed from the G_1 to the S-phase of growth, it was suggested that RR and other DNA metabolic enzymes co-localized in the nucleus forming ''replitase'', which consisted of enzymes involved both in dNTP synthesis and DNA replication [16]. However, later works cast serious doubts on the ''replitase'' concept [17]. Immunocytochemical studies had shown that both hRRM1 and hRRM2 were confined to the cytoplasm [18,19]. In a more recent study, M2B was found in the nucleus after DNA damage, and hRRM1 remained in the cytoplasm of resting cells [4]. This led to the speculation that M2B may be associated with an unidentified large-subunit protein in the nucleus to synthesize dNTPs and facilitate DNA repair. R1 (analogous to M1 in mouse) and R2 (analogous to M2 in mouse), which are located in the cytoplasm, synthesized the dNTPs that diffused into the nucleus for DNA replication [12]. The effects on the dNTPs pool by perturbation of DNA synthesis can be explained by allosteric enzyme regulation and substrate cycling [2]. Several nucleoside transporter (NT) proteins were reported to play an essential role for nucleoside transportation between cell membranes [20]. Whether dNTPs can diffuse freely through the nuclear pore remains unclear. Moreover, accumulation of RR subunits in the nucleus has never been directly demonstrated in mammalian cells in physiological conditions.

In this study, we investigated M2B expression in a synchronized study, which was associated with cyclin E expression. We used living cell sorting, Western blots, and enzymatic activity to confirm the expression of M2B at G_1/S-phase transition. The M2B subunit can translocate from the cytoplasm to the nucleus in response to DNA replication. We also incubated KB cells with M2B-shRNA. Here, we report the expression level of M2B that influences S-phase transition.

2. Materials and methods

2.1. Cell culture, plasmid and transfection

The human oropharyngeal epidermal carcinoma cell line KB was purchased from the American Type Culture Collection (ATCC). Cells were grown in RPMI 1640 medium supplemented with 10% fetal bovine serum (FBS) and 1% penicillin–streptomycin.

The fragments of 5′ AATGCTGTTCGGATAGAACAG 3′ (927–947, GenBank™ accession number BC001886) and 5′ AATTGAAACCATGCCCTATGT 3′ (718–738 GenBank™ accession number AB036063) were designed for construction of hRRM2-shRNA and M2B-shRNA, respectively. The fragment 5′ AGGTCGACTT ATCAAAGGATC 3′ was inserted to construct scramble shRNA. The shRNA fragments were separated with a 7-nucleotide spacer (TCAAGAG). Double-stranded DNA oligonucleotides encoding shRNA were ligated into the *Bbs*I site of the psiRNA–hH1GFPzeoG2 vector (InvivoGen) to construct short hairpin small interference RNA (shRNA) expression vectors. The details of shRNA vector construction has been described in our published paper [21].

About (1–3) $\times 10^6$ cells were trypsinized and washed with Hypoosmolar electroporation buffer (Eppendorf). Cell pellets were resuspended and brought to a final volume of 400 μl in electroporation buffer containing 10 μg of the target plasmid DNA. The cell suspension was placed in an electroporation cuvette (2 mm gap, Eppendorf). Electroporation was done for 100 μs at 800 V.

2.2. Nuclei isolation and nuclear protein extraction

Nuclei isolation was optimized from Ref. [22]. The efficiency of the nuclei isolation was determined by a scanning electron micrograph. To isolate nuclei, 1×10^7 cultured cells were suspended in 400 ml of 10 mM HEPES (pH 7.9), 10 mM KCl, 0.1 mM EDTA, 0.1 mM EGTA, 1 mM DTT, and 0.5 mM PMSF for 15 min. 25 ml Nonidet P40 was added and cell pellets were harvested. The NP-40 buffer was removed by aspiration, and remaining cell contents were washed with PBS. A microscope was employed to check that the nuclei were isolated from whole cells.

To extract nuclear protein, the cell pellets were resuspended in 50 ml of 20 mM HEPES (pH 7.9), 0.4 M NaCl, 1 mM EDTA, 1 mM EGTA, 1 mM DTT and 1 mM PMSF;

vigorously rocked for 15 min at 4 °C, and centrifuged (10,000 rpm, 15 min, 4 °C). The supernatant was collected (approximately 55 ml) and stored at −80 °C.

2.3. Western blots assay

Each 40 μg of cell lysates were separated by 4–12% SDS PAGE, transferred to a PVDF membrane, and incubated in blocking buffer (1% I-block™ reagent and 0.1% Tween-20) with the primary antibody (1:200 dilution) for 45 min at room temperature. After five washes, the membrane was incubated with alkaline phosphatase and conjugated secondary antibody (1:2000 dilution) for 30–60 min. After sequential washes, a thin layer of CSPD Ready-to-Use substrate solution (Applied Biosystem) was transferred over each membrane, incubated for 5 min, and exposed to X-ray film for 3 min.

2.4. Flow cytometry analysis

Approximately 5×10^5 cells were fixed with 100% methanol for at least 20 min, washed with PBS, and pre-blocked with 10% BSA for 20 min at room temperature. Cells were incubated with the primary antibodies (1:100 diluted into 1.5% BSA) against hRRM1, hRRM2 and M2B for 1 h at 37 °C. After incubation, cells were washed with PBS and blocked with 1.5% BSA solution, containing 1:50 diluted FITC-labeled bovine anti-goat secondary antibody, at 37 °C for 45 min. After the PBS wash, cells were incubated with a propidium iodide (PI)/Triton X-100 staining solution (0.1% of Triton X-100, 0.2 mg/ml of RNase A and 1 mg/ml of PI), for 30 min at room temperature. The samples were measured at an emission wavelength of 520 nm and an excitation wavelength of 488 nm for FITC, and an emission wavelength of 615 nm and an excitation wavelength of 530 nm for PI. ModiFit LT 3.0 (Verity Software Products) and Summit v3.1 (Cytomation) were utilized to analyze the cell cycle and protein signals of RR subunits.

2.5. The [^{3}H] labeled CDP incorporation assay and in vitro RR activity assay

The [^{3}H] labeled CDP incorporation assay was described in our previous study [13]. Cells (approximately 3×10^5) were plated on a 60 mm dish. To enhance cell permeability, cells were washed twice in solution [150 mM sucrose, 80 mM KCl, 35 mM HEPES (pH 7.4), 5 mM potassium phosphate (pH 7.4), 5 mM $MgCl_2$, 0.5 mM $CaCl_2$]. Permeabilized cells were incubated at 37 °C for 10 min in a 300 μl reaction containing 50 mM HEPES (pH 7.4), 0.75 mM $CaCl_2$, 10 mM phosphoenolpyruvate, 0.2 mM [^{3}H]rCDP, 0.2 mM rGDP, 0.2 mM rADP, and 0.2 mM dTDP. After incubation, 150 μl of the reaction was mixed with 30 μl of a 60% perchloric acid solution and a 0.1% Na PPi, and incubated on ice for 15 min. The pellet was extracted with 0.1 ml of 0.2N NaOH and incubated at 37 °C for 30 min. Samples were suspended and counted in 5 ml of Ecoscint A using a Beckman LS 5000CE liquid scintillation counter.

The in vitro RR activity assay has been described in detail [23]. Cell extracts were passed through a Sephadex G25 spin column to remove endogenous nucleotides. The reaction mixture contained 0.15 μM of [^{3}H]-CDP, 50 mM of HEPES (pH 7.2), 6 mM of DTT, 4 mM of magnesium acetate, 2 mM of ATP, and 0.05 mM of CDP, and a specific amount of cell lysate. Mixtures were incubated at 37 °C for 20 min. The formed dCDP and remaining CDP were dephosphorylated by phosphodiesterase. Cytidine and deoxycytidine were separated using a C18 ion exchange HPLC column.

2.6. Confocal microscopy

We have described the protocol for confocal microscopy analysis in our previous study [8,13]. Specimens were incubated with 2 μg/ml primary antibodies for 60 min. After three washes, cover slips were incubated with FITC-conjugated goat anti-rabbit (5 μg/ml) or rhodamine-conjugated bovine anti-goat (5 μg/ml) secondary antibodies, in a dark chamber for 45 min, and then washed three times with PBS. Cover slips were mounted and examined with a confocal microscope using the appropriate filters.

2.7. dNTPs pool assay

An optimized dNTP pool assay has been described in our previous study [23]. About 1×10^6 cell pellets were harvested and added to 100 μl of 15% trichloroacetic acid. Supernatants were saved and extracted with two 50 μl aliquots of 1,1,2-trichlorotrifluoroethane/trioctylamine (55:45). The reaction mixture (50 μl) of the assay contained 50 mM of Tris–HCl (pH 7.5), 10 mM of $MgCl_2$, 5 mM DTT, 0.25 μM of [^{3}H]-dATP (for dCTP, dGTP and dTTP pool detection) or [^{3}H]-dTTP (for dATP pool detection), 0.2 units of sequenase, and a diluted sample. After a 20 min incubation, 40 μl of aliquots were applied to circular Whatman DE81 ion exchange papers. After three washes, samples were counted in a liquid scintillation counter and compared to a standard sample prepared in the presence of 0, 0.25, 0.50, 0.75 and 1.0 pmol/μl of each dATP, dTTP, dGTP and dCTP.

2.8. Real-time cell proliferation monitoring system

The ACEA RT-CES™ was used to monitor cell growth in real time [24]. This system uses microelectronic cell sensor arrays that are integrated into the bottom of microtiter plates. The electrode resistance was measured every 30 min. To quantify cell status based on the measured cell electrode impedance, the parameter, cell index (CI) is derived

according to $CI = \max_{i=1,\ldots,N}(\text{Rcell}(fi)/\text{Rb}(fi) - 1)$, where Rcell($fi$) and Rb($fi$) are the frequency-dependent electrode resistances (a component of impedance) in the presence or absence of cells, respectively. N is the number of the frequency points at which the impedance is measured. CI is a relative value to indicate how many cells attached to the electrodes. The slope of the CI curve reflects the growth speed of cells.

3. Results

3.1. Alteration of M2B expression in serum synchronized study

To investigate the role of M2B in cell proliferation without DNA damage, KB cells were synchronized using serum starvation. After starvation for 96 h in 0.2% FBS medium, 75%, 18%, and 7% of KB cells were distributed at the G_1/G_0, S, and G_2 phase, respectively (time 0, Fig. 1A). When 10% FBS medium was added back to these cells, the percentage of S-phase cells increased from 18% at 0 h to 43% at 12 h, and subsequently decreased over the next 10 h. Conversely, the G_1/G_0 cells decreased from 0 to 12 h post-supplementation, then recovered. The percentage of G_2/M-phase cells increased during 8–14 h post-supplementation, peaked at 14–16 h, and declined gradually over the next 8 h of the assay (Fig. 1A).

Cyclin A, B1, and E, the family of proteins implicated in the induction and control of cellular mitosis, were employed as cell cycle indicators. Cyclin A expression levels increased steadily after the serum supplement and peaked at 14 h (Fig. 1B), which is compatible with data regarding the percentage of cells in the G_2-phase (Fig. 1A). Cyclin B1, which increases during G_2 and peaks at the M phase, rose at 10 h and maintained a high level of expression afterwards. Cyclin E increased at 4 h after serum addition, and peaked at 8 h, which indicated the G_1/S transition phase. There were high levels of hRRM2 expression between the 8 and 18 h. In contrast, M2B levels peaked at 6 h after serum addition, then declined steadily (Fig. 1B). These results indicate that M2B increases prior to hRRM2 in response to serum addition.

3.2. Highest expression of M2B at G_1/S-phase transition

To avoid serum-related artifacts and confirm that alterations of RR subunits were associated with physiological cellular turn over, unstressed KB cells were analyzed using flow cytometry. As the amount of DNA increased in these cells, signals of the hRRM1, hRRM2, and M2B subunits first increased sharply, then flattened and decreased slightly (Fig. 2A). The background signal of all the samples without primary antibody or without FITC conjugated secondary antibody staining increased linearly with the DNA. The cells were divided into 10 subgroups between DNA signal values of 64 and 192. The expression S_i of the RR subunits was adjusted with the background $S_{(BG)}$ value of each subgroup. The curves (Fig. 2B) for RR subunit levels in

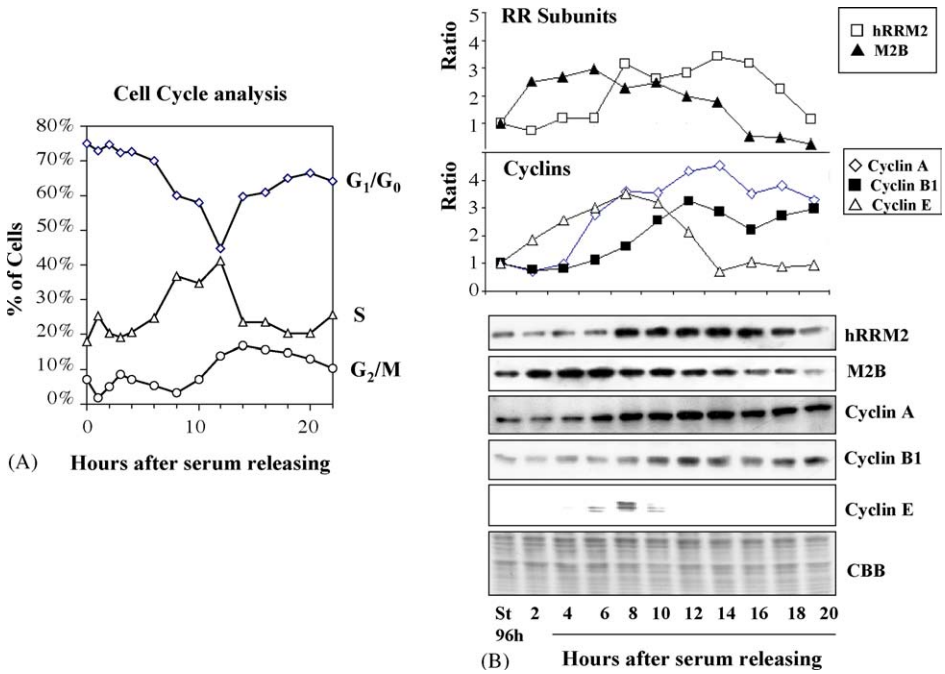

Fig. 1. Cell cycle distribution and RR subunit expression in response to serum release in starved KB cells. The KB cells were starved with 0.2% serum medium for 96 h and then released in 10% serum medium. (A) Cell cycle analysis: the cells were harvested at 2 h intervals after release. Flow cytometry was employed to detect the DNA signal and Modifit LT 3.0 was applied to analyze cell cycle distribution. (B) Western Blot assay: antibodies against RR subunits and cyclins were used to detect corresponding protein expression. Coomassie blue stain (CBB) was employed as the loading control.

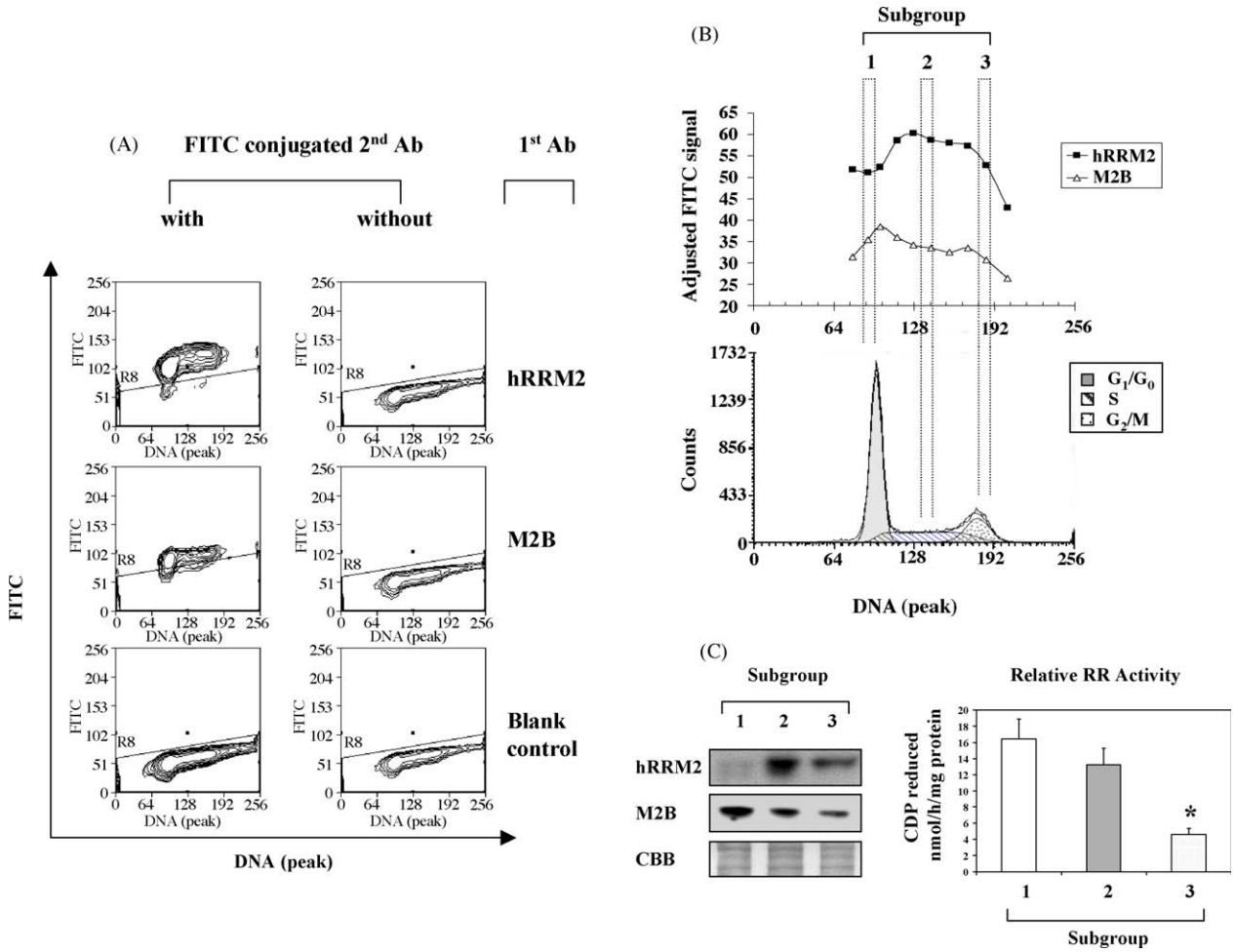

Fig. 2. Expression of RR subunits contributes to RR activity in cell cycle. (A) KB cells were incubated with primary antibodies (goat) of anti-hRRM1, anti-hRRM2, and anti-M2B. A sample without the first antibody was employed as a blank control. Samples were blotted with or without FITC conjugated bovine anti-goat secondary antibody. The FITC signal without secondary antibody was regarded as background value. The PI stain was used to indicate quantity of DNA. (B) Cells were assembled into 10 subgroups based on distribution of DNA quantities from 64 to 192. The signal value of FITC for each subgroup was adjusted by corresponding with the background value using the equation: $S_i = \sum_j S_{(\mathrm{FITC})j}/n_j - \sum_j S_{(\mathrm{BG})j}/n_j$, where S_i is the adjusted value for each subgroup cells; $S_{(\mathrm{FITC})}$ the crude value, $S_{(\mathrm{BG})}$ the background value, and n is the number of cells. The adjusted value curves were in vertical alignment with DNA distribution pattern. KB cells were sorted to subgroups 1–3 according to DNA quantities. (C) Lysates extracted from the sorting cells were utilized to perform Western analysis (left panel). The RR activities were detected using CDP reducing assay (right panel); asterisk (*) indicates difference between subgroup 3 and subgroup 1 is statistically significance (Student's t-test, $n = 3$, $p < 0.05$).

the cell cycle were calculated from data in Fig. 2A, according to the equation in Fig. 2 legend. hRRM2 is an S-phase-specific protein that increased only at the S-phase and decreased when the cell progressed into the G_2/M-phase. The M2B subunit increased at the G_1/S-phase transition and decreased between the later S-phase and G_2/M-phase. The above results have been further confirmed in COS-1 and PC3 cell lines (data not shown).

To further quantify RR subunit expression in physiological growth conditions, flow cytometry was employed to sort living KB cells into subgroups 1–3 based on different cell DNA amounts (Fig. 2B). In subgroup 1, the majority of cells were in the G_1/G_0 phase, including small amounts of pre-S and earlier S-phase cells. Subgroup 2 contained mid-S-phase cells, and subgroup 3 included later S-phase and G_2/M-phase cells. The protein level of M2B was highest in subgroup 1, and was progressively lower in subgroup 2 and subgroup 3 (Fig. 2C, left panel). hRRM2 had its highest expression during mid-S phase, but was barely detectable in G_1/G_0 and earlier S-phase cells. The RR enzymatic assay was standardized by protein amount. Relative RR activity of subgroup 1 and 2 cell lysates was significantly higher than that of subgroup 3 (Fig. 2C, right panel).

3.3. Nuclear localization of RR subunits in response to cell proliferation

Confocal microscopy allowed us to examine the subcellular localization of RR subunits in normal growth cells and determine that these subunits were mainly distributed in the cytoplasm, but a few cells had RR subunits primarily located in the nucleus (Fig. 3A).

After serum starvation for 96 h, almost all RR subunits were predominantly localized in the cytoplasm, but 2 h

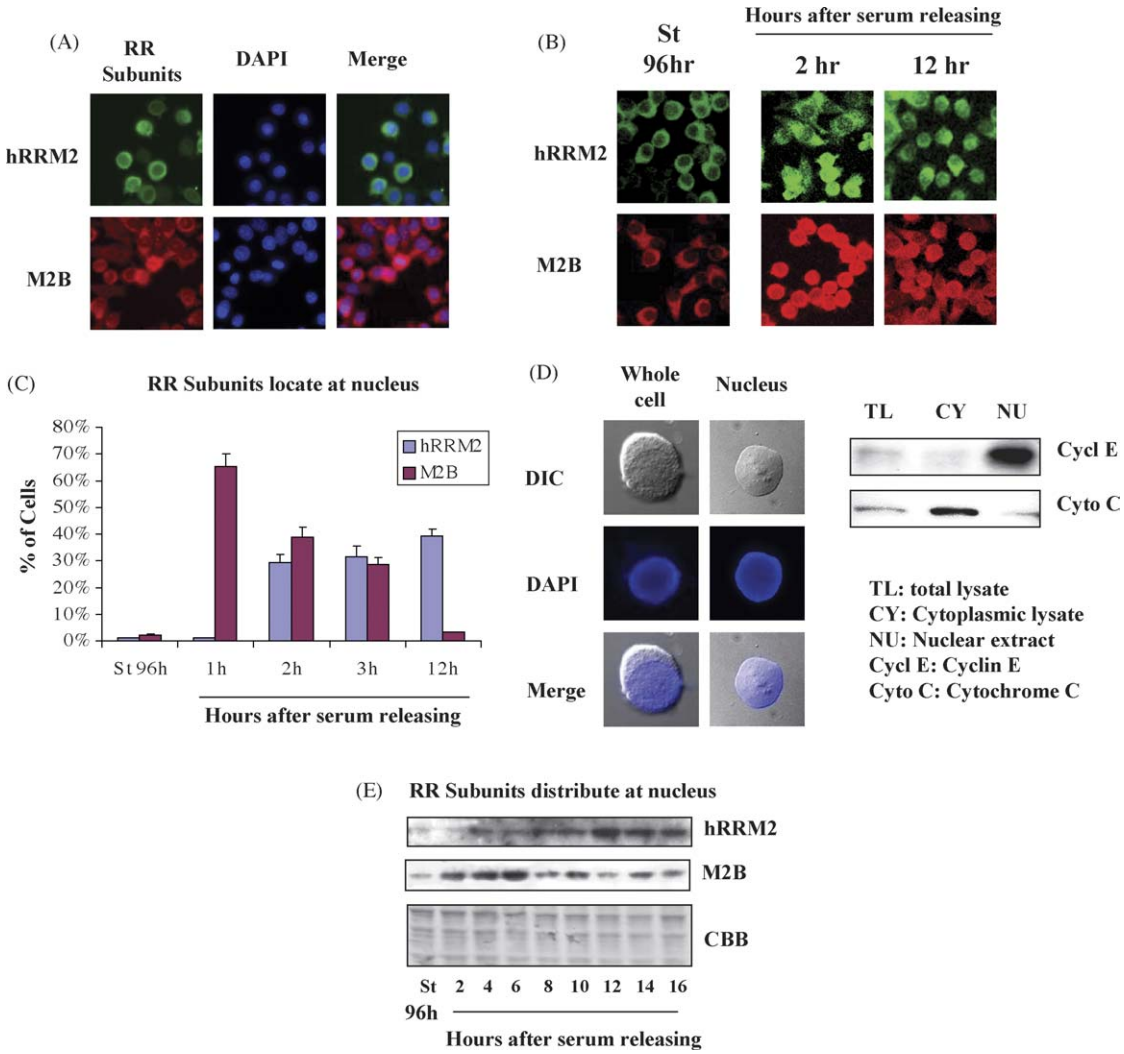

Fig. 3. The RR Subunits redistributed from cytoplasm into nucleus in response to cell proliferation. (A) Normal growth cells were harvested and stained with hRRM1, hRRM2, and M2B antibodies. hRRM1 and M2B were visualized with rhodamine-conjugated bovine anti-goat antibody; hRRM2 was visualized with FITC-conjugated goat anti-rabbit antibody. DAPI was employed to stain the nucleus. (B) The KB cells were synchronized by 0.2% FBS medium for 93 h, then either immediately fixed as negative control (first line), or returned to 10% FBS medium for 2 and 12 h (second and third line). (C) Quantification of RR nuclear subcellular localization was done using the entire field of vision for each experiment. Percentages of cells with predominantly nuclear signal were calculated. (D) Left panel: differential interference contrast (DIC) images of whole KB cells and isolated nuclei; DAPI staining indicates the nucleus. Right panel: 40 μg of protein extract of whole cell (TL), cytoplasm (CY) and nucleus (NU) were loaded and blotted with anti-cytochrome *c* and anti-cyclin E antibodies. (E) Nuclear accumulation of RR subunits: the nuclei isolation was described in Section 2. Forty micrograms of nuclear extracts were loaded onto gels. Antibodies against hRRM1, hRRM2, and M2B were used to detect corresponding protein expression. Coomassie blue stain (CBB) was the loading control.

after addition of 10% serum media, RR subunits could be seen in the nucleus (Fig. 3B). In Fig. 3B, the cells with M2 located at the nucleus steadily increased from 1% at 0 h to 39% at 12 h. However, cells expressing nuclear M2B increased from 2% at 0 h to 65% at 1 h after serum addition, and gradually decreased to 3% after 12 h.

To confirm this finding, Western blot analysis was employed to investigate the RR subunits accumulated at nucleus fraction. The efficiency of nuclear extraction is described in Fig. 3D. Nuclear integrity was preserved, as viewed with differential interference contrast microscopy (Fig. 3D, left panel). In addition, cyclin E (a nuclear protein) and cytochrome *c* (a mitochondrial protein) were dominantly distributed at nuclear (NU) and cytoplasmic (CY) fractions, respectively (Fig. 3D, right panel). Western blot analysis revealed that M2B protein levels peaked at 6 h (Fig. 3E). hRRM2 was barely detectable immediately after serum starvation, but increased to its highest level at 12 h. These results indicate that RR subunits M2 and M2B translocated from the cytoplasm to the nucleus in response to serum addition, and that M2B subunits translocated before hRRM2.

3.4. Dynamic changes of dNTPs pool in response to DNA replication

RR is one of the key enzymes involved in providing dNTPs for DNA replication and repair. After serum

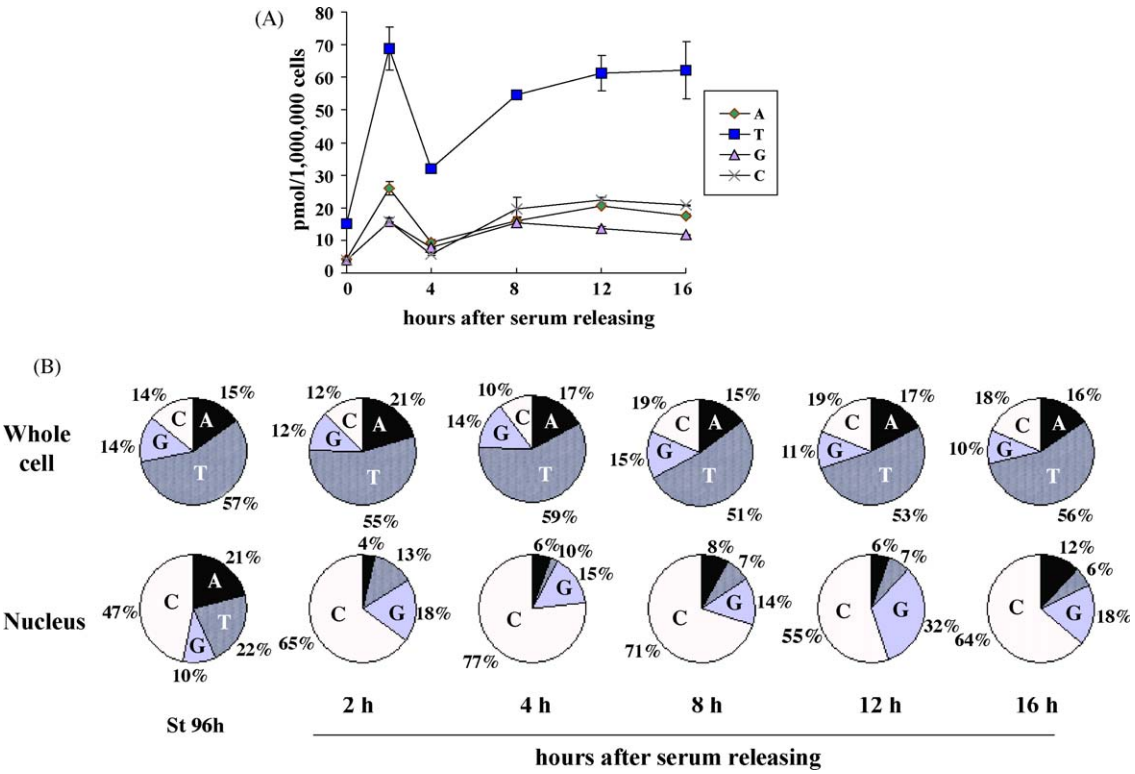

Fig. 4. Dynamic change of dNTP pool in response to serum release in starved KB cells. The KB cells were starved with 0.2% serum medium for 96 h and then were re-cultured in 10% FBS serum medium for 2, 4, 8, 12 and 16 h. After harvesting, cell numbers were counted. The dNTPs pool assay is described in Section 2. Each sample measurement was repeated three times. (A) Dynamic change of dNTPs' concentrations in response to DNA replication. (B) Dynamic change of dNTPs' proportion in the nucleus and whole cells after serum releasing.

starvation, all dNTPs had a relatively low concentration (Fig. 4A). When cells were supplemented with serum, dNTP concentration increased significantly at 2 h and subsequently declined at 4 h. Total dNTPs proceeded to increase steadily from 4 to 12 h and to decrease slightly at 16 h. Expansion of the dNTP pool and increase of M2B at early periods indicate that M2B may play a dominant role in providing dNTPs for the G_1- to S-phase transition.

The proportions of dATP, dTTP, dGTP, and dCTP in starved KB cells are 15.4%, 56.3%, 14.1%, and 14.2%, respectively and these proportions change very little with the addition of serum (Fig. 4B, upper panel). dTTP is the most dominant deoxyribonucleotide in the whole cell, while, the changes of dNTPs in the nucleus differ from that of the whole cell (Fig. 4B, lower panel). The proportions of dATP, dTTP, dGTP, and dCTP in the nucleus of starved KB cells are 21.1%, 22.0%, 9.9%, and 47.1%, respectively. However, in the nucleus, dCTP is most dominant. After serum is supplemented to starving KB cells, the proportion of dATP and dTTP in the nucleus is significantly reduced from 2 to 16 h, while the proportion of dCTP is significantly increased in the nucleus. The above findings indicated that the nuclear localization of RR subunits was associated with dynamic changes of nuclear dNTPs' proportion after serum was re-added.

3.5. Expression of RR subunit M2B is associated with cell proliferation ability

The above finding implied that down-regulation of RR small subunits M2B and hRRM2 might reduce the speed of cell growth. shRNA expression vectors were employed to reduce M2B and hRRM2 expression in KB cells (Fig. 5A). Under the same condition as electroporation, flow cytometry analysis of green fluorescence protein control vector indicated the transfection efficiency was 80–90% in KB cells. In Fig. 5B, hRRM2-shRNA and M2B-shRNA2, rather than scramble shRNA, could specifically inhibit hRRM2 and M2B expression levels to 40% and 20%, respectively. Determination of dNTPs pool validated that the dATP, dCTP, dGTP and dTTP concentration has been reduced from 4.13, 3.81, 3.79 and 15.08 pmol/1,000,000 cells in vector control to 2.12, 2.32, 2.01and 8.93 pmol/1,000,000 cells in M2B-shRNA and 1.51, 1.83, 1.95 and 9.56 pmol/1,000,000 cells in hRRM2-shRNA transfectants, respectively (Fig. 5C). Flow cytometry analysis of the distribution of cell cycles shows that low expression of hRRM2 and M2B cells inhibited by shRNA expression vectors would prevent cells from progressing into the S-phase (Fig. 5D). Compared to the shRNA control vector, cell growth curves were flatter when KB cells were transfected with M2-shRNA and M2B-shRNA2 (Fig. 5E). In addition, similar results were obtained from a time-point

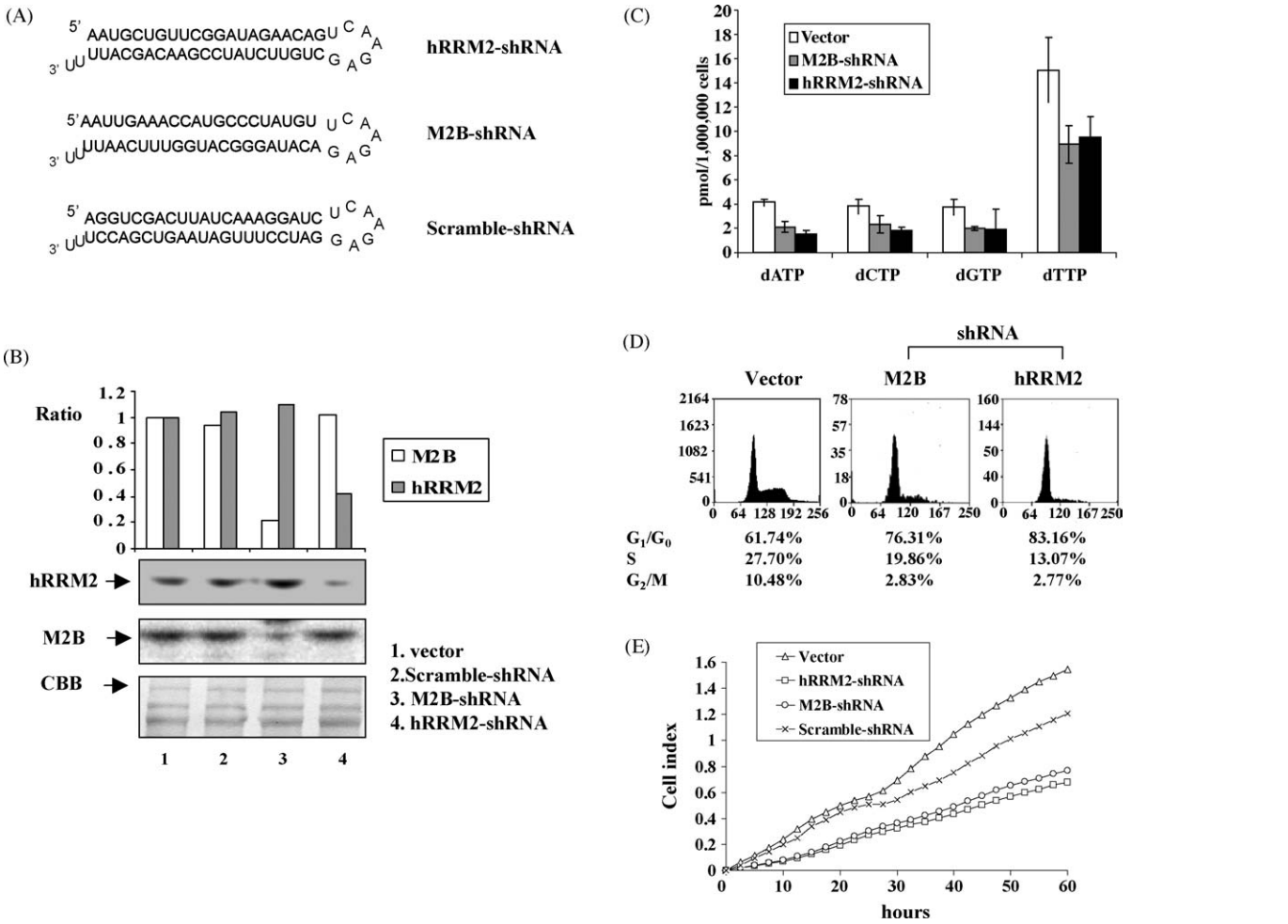

Fig. 5. Expression of RR small subunits is correlated with cell proliferation index. (A) Construction of shRNA expression vectors was described in Section 2. (B) Ten micrograms of shRNA vectors and a control vector were transfected into 1×10^6 normal growth KB cells using electroporation. Cells were harvested after electroporation for 24 h. Western blot shows inhibition of shRNA expression vectors. (C) dNTP pool determination: transfectants were incubated and harvested at 48 h. Harvested cells were detected for dATP, dCTP, dGTP and dTTP concentrations, respectively. The dNTPs were adjusted by cells number counting. (D) The harvested cells were fixed and the cell cycle distribution was analyzed using flow cytometry. (E) After transfection with hRRM2-shRNA, M2B-shRNA and control vector for 24 h, 1×10^4 cells were seeded onto wells of 16× microtiter plates. Cell growth was monitored by RT-CES™ system, and showed steady increases in cell index (an indication of cell growth).

cell count study with antisense expression vectors (data not shown). It was indicated the inhibiting hRRM2 or M2B expression by using shRNA expression vector could cause growth retardation in KB cells.

4. Discussion

In mammalian cells, the RR small subunit hRRM2 (R2) have been known to provide dNTPs for DNA replication [7,25,26]. The human RR small subunit M2B is thought to contribute to DNA repair in response to DNA damage [4,9,13]. Our study shows that the expression and localization of M2B is highly regulated during the physiological cell cycle. Under non-DNA damage conditions, M2B coordinated with cyclin E, which has the highest expression at the G_1/S-phase transition. In addition, M2B rapidly redistributed from the cytoplasm to the nucleus in response to DNA replication signaling. Nuclear accumulation of M2B is earlier than hRRM2 during DNA synthesis (Fig. 3). RR subunit M2B accumulated to maximum levels at the G_1/S-phase transition, and degraded steadily when cells turned into the S-phase. These evidences indicate that the accumulation and nuclear localization of M2B may be involved in providing dNTPs at the G_1/S-phase transition to play a pivotal role in initiating DNA synthesis in KB cells under physiological growth conditions.

There are two opinions on where deoxyribonucleotide (dNTP) synthesis possibly occurs. The ‘‘replitase’’ model indicates that NDPs, rather than free dNTPs, are ‘‘channeled’’ directly into DNA synthesis in the nucleus [16,27–29]. However, hRRM1 and hRRM2 can only be seen in the cytoplasm in immunohistochemistry staining studies. This observation opposes the previous view in proposing that dNTPs may be synthesized in the cytoplasm and diffused into the nucleus for DNA incorporation [12]. DNA replication requires much more dNTPs than DNA repair. Interestingly, the expansion of the dNTP pool in DNA damaged

cells is much higher than that of the S-phase cells [17,30]. In the diffusion model, this effect is because DNA polymerase requires a higher concentration of dNTPs in DNA repair [30–32]. Nevertheless, the diffusion model hardly explains why rNDP is much more efficient than dNTP in its incorporation into DNA [33,34]. In budding yeast, the small subunits RNR2 and RNR4 redistribute from the nucleus to the cytoplasm under hydroxyurea and methyl methanesulfonate treatment [3]. In KB cells, both hRRM2 and M2B can translocate into the nucleus after UV irradiation and re-supplementing the serum. The different results yielded may be due to the dissimilarity in individual treatments and specimens. The above results indicate that the subunits of RR can translocate between the cytoplasm and the nucleus in both yeast and mammalian cells. In addition, our study demonstrated that nuclear localization of RR subunits was associated with dynamic changes of nuclear dNTPs' proportion at the G_1/S-phase transition. It needs to be further demonstrated whether hRRM2 and M2B form a holoenzyme in the nucleus to directly provide dNTPs.

Regulation of RR subunits' translocation plays a crucial role in regulating RR activity for DNA replication and DNA repair. How the signals of DNA replication and repair are conducted to initiate RR translocation is mainly unknown. However, the nuclear localization sequence (NLS) is required for larger proteins to enter the nucleus [35]. The NLS of RR subunits has not yet been identified. Recent studies showed that NLS-dependent nuclear localization was precisely regulated and coupled with phosphorylation in SV40 and STAT1 [36,37]. The phosphorylation sites, together with the NLS, constitute phosphorylation-mediated regulatory modules for nuclear localization. The mouse R2 serine-20 residue can be phosphorylated by p34cdc2 kinase without affecting RR activity [38,39]. The additionally modified M2B large band has been detected on CEM cells and its drug resistant clones [40]. It is implied that protein modification plays a critical role in M2B translocation in response to DNA replication and repair. However, the detailed mechanism regarding the signaling of DNA replication and repair to RR subunit migration into the nucleus needs further investigation.

The cell cycle-dependent expression of RR subunits can be observed in both p53 wild-type cell lines (KB and COS1) and the p53 mutated cell line (PC3) (data not shown). The translocation of M2B can also be observed in p53 mutant PC3 cells [8]. The mechanism of replication arrest at the G_1/G_0-phase by the RR inhibitor (HU) is not dependent on the Mec1/Rad53 pathway in yeast [41]. Redistribution of RNR2 and RNR4 is also independent of Rad53 transcriptional induction [3]. It was implied that the expression and translocation of M2B in DNA replication might be independent of the p53 pathway.

Previous studies demonstrated that the replication rate at the replication fork in mammalian cells is not constant throughout the S-phase of the cell cycle [42,43]. Actively transcribed genes usually replicate during the first quarter of the S-phase [43,44]. Exogenous dNTPs accelerates the replication process at early S-phase rather than late S-phase [45]. RR is a critical enzyme involved with providing dNTPs for DNA replication. Insufficient dNTP pools would prevent cells escaping from the G_1- to S-phase [41]. Impairment of M2B can cause severe renal failure, growth retardation and early mortality in Rrm2b-null mice [46]. Hydroxyurea and triapine, inhibitors of M2B and hRRM2, could decrease the dNTP pool and cause KB cell arrest at the G_1-phase (data not shown). A recent study demonstrated that RNAi-mediated M2B reduction selectivity inhibited growth and enhanced chemosensitivity in cancer cell lines rather than in normal fibroblasts [47]. Our study yielded similar results when using the M2B-shRNA expression vector. Using M2B-shRNA, the M2B protein could be reduced to 20% level, which results in 50% decrease of dNTPs in transfectant (Fig. 5B and C). Inhibition of cell proliferation by M2B-shRNA might be due to insufficient dNTPs that provided for initiation of DNA replication at early S-phase. Our recent immunochemistry study showed that p53R2 over-expressed various cancer tissue rather than corresponding normal tissue. It was suggested that M2B might be a potential target for chemotherapeutic agents in the future.

Acknowledgements

This was a NIH Grant (CA 72767) supported project. I would like to acknowledge Lucy Brown and Spalla Claudio for helping to run the flow cytometry, as well as Mariko Lee for conducting confocal microscopy in co-facility laboratories at City of Hope. I appreciate Kristine Justus' efforts in editing and critiquing this paper.

References

[1] Jordan A, Reichard P. Ribonucleotide reductases. Annu Rev Biochem 1998;67:71–98.
[2] Reichard P. Interactions between deoxyribonucleotide and DNA synthesis. Annu Rev Biochem 1988;57:349–74.
[3] Yao R, Zhang Z, An X, Bucci B, Perlstein DL, Stubbe J, et al. Subcellular localization of yeast ribonucleotide reductase regulated by the DNA replication and damage checkpoint pathways. Proc Natl Acad Sci USA 2003;100:6628–33.
[4] Tanaka H, Arakawa H, Yamaguchi T, Shiraishi K, Fukuda S, Matsui K, et al. A ribonucleotide reductase gene involved in a p53-dependent cell-cycle checkpoint for DNA damage. Nature 2000;404:42–9.
[5] Rova U, Adrait A, Potsch S, Graslund A, Thelander L. Evidence by mutagenesis that Tyr(370) of the mouse ribonucleotide reductase R2 protein is the connecting link in the intersubunit radical transfer pathway. J Biol Chem 1999;274:23746–51.
[6] Elledge SJ, Davis RW. Two genes differentially regulated in the cell cycle and by DNA-damaging agents encode alternative regulatory subunits of ribonucleotide reductase. Genes Dev 1990;4:740–51.

[7] Eriksson S, Graslund A, Skog S, Thelander L, Tribukait B. Cell cycle-dependent regulation of mammalian ribonucleotide reductase. The S phase-correlated increase in subunit M2 is regulated by de novo protein synthesis. J Biol Chem 1984;259:11695–700.
[8] Zhou B, Liu X, Mo X, Xue L, Darwish D, Qiu W, et al. The human ribonucleotide reductase subunit hRRM2 complements p53R2 in response to UV-induced DNA repair in cells with mutant p53. Cancer Res 2003;63:6583–94.
[9] Yamaguchi T, Matsuda K, Sagiya Y, Iwadate M, Fujino MA, Nakamura Y, et al. p53R2-dependent pathway for DNA synthesis in a p53-regulated cell cycle checkpoint. Cancer Res 2001;61:8256–62.
[10] Yanamoto S, Kawasaki G, Yoshitomi I, Mizuno A. Expression of p53R2, newly p53 target in oral normal epithelium, epithelial dysplasia and squamous cell carcinoma. Cancer Lett 2003;190:233–43.
[11] Nakano K, Balint E, Ashcroft M, Vousden KH. A ribonucleotide reductase gene is a transcriptional target of p53 and p73. Oncogene 2000;19:4283–9.
[12] Lozano G, Elledge SJ. p53 sends nucleotides to repair DNA. Nature 2000;404:24–5.
[13] Xue L, Zhou B, Liu X, Qiu W, Jin Z, Yen Y. Wild-type p53 regulates human ribonucleotide reductase by protein–protein interaction with p53R2 as well as hRRM2 subunits. Cancer Res 2003;63:980–6.
[14] Guittet O, Hakansson P, Voevodskaya N, Fridd S, Graslund A, Arakawa H, et al. Mammalian p53R2 protein forms an active ribonucleotide reductase in vitro with the R1 protein, which is expressed both in resting cells in response to DNA damage and in proliferating cells. J Biol Chem 2001;276:40647–51.
[15] Shao J, Zhou B, Zhu L, Qiu W, Yuan YC, Xi B, et al. In vitro characterization of enzymatic properties and inhibition of the p53R2 subunit of human ribonucleotide reductase. Cancer Res 2004;64:1–6.
[16] Noguchi H, veer Reddy GP, Pardee AB. Rapid incorporation of label from ribonucleoside disphosphates into DNA by a cell-free high molecular weight fraction from animal cell nuclei. Cell 1983; 32:443–51.
[17] Reichard P. Ribonucleotide reductase and deoxyribonucleotide pools. Basic Life Sci 1985;31:33–45.
[18] Engstrom Y, Rozell B, Hansson HA, Stemme S, Thelander L. Localization of ribonucleotide reductase in mammalian cells. EMBO J 1984;3:863–7.
[19] Engstrom Y, Rozell B. Immunocytochemical evidence for the cytoplasmic localization and differential expression during the cell cycle of the M1 and M2 subunits of mammalian ribonucleotide reductase. EMBO J 1988;7:1615–20.
[20] Griffiths M, Beaumont N, Yao SY, Sundaram M, Boumah CE, Davies A, et al. Cloning of a human nucleoside transporter implicated in the cellular uptake of adenosine and chemotherapeutic drugs. Nat Med 1997;3:89–93.
[21] Zhu L, Somlo G, Zhou B, Shao J, Bedell V, Slovak ML, et al. Fibroblast growth factor receptor 3 inhibition by short hairpin RNAs leads to apoptosis in multiple myeloma. Mol Cancer Ther 2005;4:787–98.
[22] Leeds JM, Slabaugh MB, Mathews CK. DNA precursor pools and ribonucleotide reductase activity: distribution between the nucleus and cytoplasm of mammalian cells. Mol Cell Biol 1985;5:3443–50.
[23] Zhou BS, Ker R, Ho R, Yu J, Zhao YR, Shih J, et al. Determination of deoxyribonucleoside triphosphate pool sizes in ribonucleotide reductase cDNA transfected human KB cells. Biochem Pharmacol 1998; 55:1657–65.
[24] Abassi YA, Jackson JA, Zhu J, O'Connell J, Wang X, Xu X. Label-free, real-time monitoring of IgE-mediated mast cell activation on microelectronic cell sensor arrays. J Immunol Meth 2004;292:195–205.
[25] Cory JG, Sato A. Regulation of ribonucleotide reductase activity in mammalian cells. Mol Cell Biochem 1983;53/54:257–66.
[26] Engstrom Y, Eriksson S, Jildevik I, Skog S, Thelander L, Tribukait B. Cell cycle-dependent expression of mammalian ribonucleotide reductase. Differential regulation of the two subunits. J Biol Chem 1985; 260:9114–6.
[27] veer Reddy GP, Pardee AB. Multienzyme complex for metabolic channeling in mammalian DNA replication. Proc Natl Acad Sci USA 1980;77:3312–6.
[28] veer Reddy GP. Catalytic function of thymidylate synthase is confined to S phase due to its association with replitase. Biochem Biophys Res Commun 1982;109:908–15.
[29] Reddy GP, Fager RS. Replitase: a complex integrating dNTP synthesis and DNA replication. Crit Rev Eukaryot Gene Expr 1993;3:255–77.
[30] Chabes A, Georgieva B, Domkin V, Zhao X, Rothstein R, Thelander L. Survival of DNA damage in yeast directly depends on increased dNTP levels allowed by relaxed feedback inhibition of ribonucleotide reductase. Cell 2003;112:391–401.
[31] Shimizu K, Hashimoto K, Kirchner JM, Nakai W, Nishikawa H, Resnick MA, et al. Fidelity of DNA polymerase epsilon holoenzyme from budding yeast *Saccharomyces cerevisiae*. J Biol Chem 2002; 277:37422–9.
[32] Minko IG, Washington MT, Kanuri M, Prakash L, Prakash S, Lloyd RS. Translesion synthesis past acrolein-derived DNA adduct, gamma-hydroxypropanodeoxyguanosine, by yeast and human DNA polymerase eta. J Biol Chem 2003;278:784–90.
[33] Chiba P, Bacon PE, Cory JG. Studies directed toward testing the "channeling" hypothesis–ribonucleotides—DNA in leukemia L1210 cells. Biochem Biophys Res Commun 1984;123:656–62.
[34] veer Reddy GP, Pardee AB. Coupled ribonucleoside diphosphate reduction, channeling, and incorporation into DNA of mammalian cells. J Biol Chem 1982;257:12526–31.
[35] Gorlich D, Mattaj IW. Nucleocytoplasmic transport. Science 1996; 271:1513–8.
[36] Rihs HP, Peters R, Hobom G. Nuclear localization of budgerigar fledgling disease virus capsid protein VP2 is conferred by residues 308–317. FEBS Lett 1991;291:6–8.
[37] Yoneda Y. How proteins are transported from cytoplasm to the nucleus. J Biochem (Tokyo) 1997;121:811–7.
[38] Chan AK, Persad S, Litchfield DW, Wright JA. Ribonucleotide reductase R2 protein is phosphorylated at serine-20 by P34cdc2 kinase. Biochim Biophys Acta 1999;1448:363–71.
[39] Chan AK, Litchfield DW, Wright JA. Phosphorylation of ribonucleotide reductase R2 protein: in vivo and in vitro evidence of a role for p34cdc2 and CDK2 protein kinases. Biochemistry 1993;32:12835–40.
[40] Mansson E, Flordal E, Liliemark J, Spasokoukotskaja T, Elford H, Lagercrantz S, et al. Down-regulation of deoxycytidine kinase in human leukemic cell lines resistant to cladribine and clofarabine and increased ribonucleotide reductase activity contributes to fludarabine resistance. Biochem Pharmacol 2003;65:237–47.
[41] Koc A, Wheeler LJ, Mathews CK, Merrill GF. Hydroxyurea arrests DNA replication by a mechanism that preserves basal dNTP pools. J Biol Chem 2004;279:223–30.
[42] Housman D, Huberman JA. Changes in the rate of DNA replication fork movement during S phase in mammalian cells. J Mol Biol 1975; 94:173–81.
[43] Hatton KS, Dhar V, Brown EH, Iqbal MA, Stuart S, Didamo VT, et al. Replication program of active and inactive multigene families in mammalian cells. Mol Cell Biol 1988;8:2149–58.
[44] Goldman MA, Holmquist GP, Gray MC, Caston LA, Nag A. Replication timing of genes and middle repetitive sequences. Science 1984; 224:686–92.
[45] Malinsky J, Koberna K, Stanek D, Masata M, Votruba I, Raska I. The supply of exogenous deoxyribonucleotides accelerates the speed of the replication fork in early S-phase. J Cell Sci 2001;114:747–50.
[46] Kimura T, Takeda S, Sagiya Y, Gotoh M, Nakamura Y, Arakawa H. Impaired function of p53R2 in Rrm2b-null mice causes severe renal failure through attenuation of dNTP pools. Nat Genet 2003;34:440–5.
[47] Yanamoto S, Iwamoto T, Kawasaki G, Yoshitomi I, Baba N, Mizuno A. Silencing of the p53R2 gene by RNA interference inhibits growth and enhances 5-fluorouracil sensitivity of oral cancer cells. Cancer Lett 2005;223:67–76.